7. F. Courchamp, T. Clutton-Brock, B. Grenfell, *Anim. Conserv.* **3**, 277 (2000).
8. J. P. Rood, *Anim. Behav.* **39**, 566 (1990).
9. T. H. Clutton-Brock *et al.*, *J. Anim. Ecol.* **68**, 672 (1999).
10. T. H. Clutton-Brock *et al.*, *Science* **291**, 478 (2001).
11. T. H. Clutton-Brock *et al.*, *Proc. R. Soc. London Ser. B* **267**, 301 (2000).
12. T. H. Clutton-Brock *et al.*, *Anim. Behav.* **61**, 705 (2001).
13. The animals used in this study bred in semiarid grassland along the Kuruman River to the west of Vanzylsrus (26°58′S, 21°49′E) in the South African Kalahari. Topography, vegetation, and rainfall in our study area have already been described elsewhere (*22*). Data used in these analyses were collected on 11 groups of wild meerkats between 1996 and 2000. All individuals in these groups were identifiable, and over 90% could be weighed repeatedly over the course of a day by enticing them onto electronic balances with crumbs of hard-boiled egg. The pup feeding rate was the estimated amount of food (in grams) received per hour by each pup from all group members. Estimates of feeding rate were based on the number of food items of different types and sizes received per pup, multiplied by the average weight of food items of that size category (*27*). Weight gain per hour (grams per hour) was measured as the difference in the weight of an individual at the start of the day's feeding (6 to 8 a.m.) and the beginning of the middle-day rest period (11 to 12 a.m.), divided by the number of hours between. Individuals typically acquired over 80% of their total daily weight gain (the difference in weight between the start and end of the day) during the 3 to 4 hours of the morning feeding period.
14. Group size was the mean number of individuals over 3 months old in the group over the relevant period. Helper:pup ratios were the ratios of individuals over 3 months old (excluding the dominant male and female) to pups under 3 months old. Because there was no association between group size and the average size of litters born to dominants at emergence [general linear model (GLM) of 77 litters, controlling for the effects of mother identity, $F_{1,58} = 2.86$, $P = 0.096$], the ratio of helpers to pups increased in larger groups (GLM of 77 litters, controlling for group identity, $F_{1,62} = 34.29$, $P < 0.001$).
15. J. L. Brown, *Helping and Communal Breeding in Birds* (Princeton Univ. Press, Princeton, NJ, 1987).
16. A. Cockburn, *Annu. Rev. Ecol. Syst.* **29**, 141 (1998).
17. For pup:helper ratio manipulations, we carried out 18 temporary litter manipulations in which three-quarters of pups (mean reduction, 75%; range, 67 to 83%) between the ages of 30 and 45 days were temporarily removed from a breeding group at dawn and introduced to the litter of another breeding group, increasing it by a similar amount (mean, 76%; range, 50 to 150%). In one case, we removed pups and held them over the morning feeding period without introducing them to another group in order to increase our sample of temporary removals to 10. In nine introductions, pups were accepted after being inspected, and subsequently foraged with group members. In the remaining nine, group members either showed aggression to introduced pups (in seven cases) or the pups immediately realized that they were in unusual circumstances and ran around calling instead of foraging (in two cases). These pups were immediately returned to their original group and were accepted without problem in both cases. Pups that were accepted by their "foster" groups were left with the group into which they were introduced until the end of the morning feeding period (around 4 hours later) and then returned to their original groups, in all cases without difficulty.
18. Pups that were accepted by their temporary foster groups were fed as frequently by group members as were the group's own pups [paired t test (t_8) = –1.52, $P = 0.17$), although the morning weight gain of introduced pups was lower than that of the group's own pups ($t_8 = -2.61$, $P = 0.03$). Pups and all other group members were weighed at the beginning and end of the introduction with the use of standard techniques, and these weights were used to calculate weight gains per hour (P values here are two-tailed because there was no basis for predicting the outcome of these tests in advance).
19. M. B. Manser, G. Avey, *Behav. Ecol. Sociobiol.* **48**, 429 (2000).
20. Weight as juveniles and adults was the average of the mean morning weights of individual pups at 3 to 4 months (mean, 6.3 measures per individual) and at 12 to 13 months (mean, 5.7 measures per individual).
21. For pup feeding experiments, in 11 litters with an average size of 3.4 pups per litter, we randomly assigned half the pups in each litter to an experimental group and fed each of these pups with about 12 g of hard-boiled egg at the end of morning and evening activity periods. The other pups in the litter received no additional food. Sample sizes in these analyses were the number of fed and unfed pups, and tests shown are based on GLMs controlling for sex and repeated measures within litters. Pup feeding was maintained until the animals were 60 days old, and the frequency with which they were fed by helpers had started to fall (*27*).
22. N. G. Solomon, L. L. Getz, in *Cooperative Breeding in Mammals*, N. G. Solomon, N. G. French, Eds. (Cambridge Univ. Press, Cambridge, 1997).
23. J. Lindström, *Trends Ecol. Evol.* **14**, 34 (1999).
24. A. S. Griffin, thesis, University of Edinburgh (1999).
25. T. H. Clutton-Brock *et al.*, *Science* **284**, 1577 (1999).
26. S. Creel, N. M. Creel, *The African Wild Dog: Behavior, Ecology and Conservation* (Princeton Univ. Press, Princeton, NJ), in press.
27. P. N. M. Brotherton *et al.*, *Behav. Ecol.* **12,** 590 (2001).
28. T. H. Clutton-Brock *et al.*, *Proc. R. Soc. London Ser. B.* **265**, 185 (1998).
29. R. Woodroffe, *J. Zool.* **250**, 113 (2000).
30. GENSTAT 5.4.1. (Lawes Agricultural Trust, Rothamstead Experimental Station, Hertfordshire, UK, 1998).

31. We thank Mr. and Mrs. H. Kotze for permission to work on their land at Van Zyl's Rus. The study would not have been possible without the support of members of the Mammal Research Institute, University of Pretoria (including J. Skinner, J. du Toit, and M. Haupt), and of over 40 assistants, students, postdocs, and visitors who contributed to data collection. In planning and carrying through the work, we benefited from the guidance of D. Macdonald, M. Manser, and S. Creel. Funded by grants from the Natural Environmental Research Council and the Biotechnology and Biological Sciences Research Council.

3 April 2001; accepted 4 June 2001

Loss of Caveolae, Vascular Dysfunction, and Pulmonary Defects in Caveolin-1 Gene-Disrupted Mice

Marek Drab,[1,2] Paul Verkade,[1] Marlies Elger,[3] Michael Kasper,[4] Matthias Lohn,[2,3] Birgit Lauterbach,[2,3] Jan Menne,[3] Carsten Lindschau,[2,3] Fanny Mende,[1] Friedrich C. Luft,[2] Andreas Schedl,[5] Hermann Haller,[3] Teymuras V. Kurzchalia[1]*

Caveolae are plasma membrane invaginations that may play an important role in numerous cellular processes including transport, signaling, and tumor suppression. By targeted disruption of caveolin-1, the main protein component of caveolae, we generated mice that lacked caveolae. The absence of this organelle impaired nitric oxide and calcium signaling in the cardiovascular system, causing aberrations in endothelium-dependent relaxation, contractility, and maintenance of myogenic tone. In addition, the lungs of knockout animals displayed thickening of alveolar septa caused by uncontrolled endothelial cell proliferation and fibrosis, resulting in severe physical limitations in caveolin-1–disrupted mice. Thus, caveolin-1 and caveolae play a fundamental role in organizing multiple signaling pathways in the cell.

Caveolae are characteristic flask-shaped invaginations of the plasma membrane with a diameter of 50 to 100 nm. They are present on many cell types, including endothelial cells, smooth muscle cells, and adipocytes (*1*, *2*). Fifty years after the discovery of caveolae (*3*), their function is still controversial and may include transcytosis of solutes through endothelial cells (*4*), cholesterol transport (*5*), potocytosis (*6*), signal transduction (*2*, *7*), and tumor suppression (*8*). VIP21/caveolin-1 (cav-1), a protein of 21 to 22 kD, is so far the best biochemical marker for caveolae (*9*, *10*). This integral membrane protein is a member of the caveolin-gene family, binds cholesterol (*11*), and forms high molecular weight oligomers (*12*).

To address the role of cav-1 on caveolae formation and its effect on signal transduction, we generated mice lacking the cav-1 gene by excision of exon-3 (Fig. 1A) (*13*). This encodes the transmembrane domain, the palmitoylation sites, and the so-called

[1]Max Planck Institute for Molecular Cell Biology and Genetics, Pfotenhauer-Strasse 108, D-01307 Dresden, Germany. [2]Franz Volhard Clinic and Max-Delbrück-Center for Molecular Medicine, Humboldt University Berlin, Wiltberg-Strasse 50, D-13125 Berlin, Germany. [3]Hannover Medical School, Karl-Neuberg-Strasse 1, D-30625 Hannover, Germany. [4]Institute of Anatomy, Technical University of Dresden, Fetscher-Strasse 74, D-01307 Dresden, Germany. [5]Max-Delbrück-Center for Molecular Medicine, Robert-Roessle-Strasse 10, D-13125 Berlin, Germany.

*To whom correspondence should be addressed. E-mail: kurzchalia@mpi-cbg.de

scaffolding domain of the protein. The disruption of the cav-1 gene resulted in the complete absence of caveolae in endothelial and epithelial cells of lung tissue from knockout mice (Fig. 2, C and D). In wild-type animals, abundant caveolae were present in these cells (Fig. 2, A and B). The lack of caveolae was observed in all organs analyzed, i.e., lung, adipose tissue, diaphragm, kidney, and heart. Thus, cav-1 is essential for caveolae formation, in agreement with the observation that ectopic expression of cav-1 is sufficient to induce caveolae in cells lacking this organelle (*14*). Occasionally, we detected invaginations with an electron-dense diaphragm at their neck in the large vessels (Fig. 2E), suggesting a possible morphologically distinct minor variety of cav-1–independent invaginations generated perhaps by caveolin homologs or other proteins.

We analyzed the expression of cav-1 homologs cav-2 and cav-3 in knockout mice. Although the cav-2 transcript was present in cav-1$^{-/-}$ mice, the protein could not be detected in the lungs (Fig. 1D). Similar results were obtained with other tissues including adipose, where cav-2 is normally most abundant. Because cav-1 and cav-2 form hetero-oligomers (*15*), this suggests that cav-2 in the absence of cav-1 may be degraded. In contrast, the expression of the muscle-specific cav-3 was normal in cav-1$^{-/-}$ animals.

Cav-1 is one of the major protein constituents of the plasma membrane cholesterol-enriched microdomains (rafts) (*16*, *17*). This prompted us to study whether the absence of cav-1 and cav-2 affected the contents of rafts isolated by an established procedure (*18*). Neither the pattern of protein expression (Fig. 1E) nor the lipid composition of rafts from knockout animals showed appreciable differences compared with that of the wild type. Moreover, glycosyl phosphatidylinositol (GPI)–anchored proteins, which are enriched in rafts (*19*), displayed a similar pattern in both preparations, as revealed by an aerolysin overlay (*20*) (Fig. 1E).

One of the first functions suggested for caveolae was the trancytosis of macromolecules through endothelial cells (*4*, *21*). Caveolae constitute as much as 30% of the total endothelial cell surface in capillaries. However, despite the complete loss of caveolae from the capillary network, the albumin concentration in cerebrospinal fluid, which was presumed to depend on transport through caveolae, was not different in knockout and wild-type animals (*22*). Cav-1$^{-/-}$ mice did not express any visible signs of disturbed extravascular oncotic pressure (a component of osmotic pressure that depends on the transport of albumin across the endothelium). Thus, transcytosis occurs through, or is compensated for by, an alternative pathway. Caveolin also has been suggested to play a role in cholesterol transport (*23*). However, the blood lipoprotein composition and the cholesterol content of high-density lipoprotein were

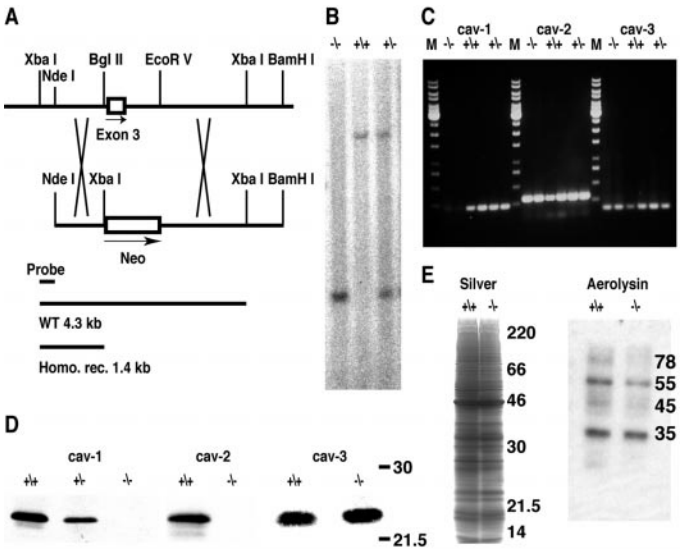

Fig. 1. Generation of caveolin-1–deficient mice. (**A**) Schematic representation of the genomic caveolin-1 locus and the targeting vector. Positions of restriction enzyme sites and of the probe used for Southern (DNA) analysis are shown. (**B**) Southern blot analysis of genomic DNA from three littermate progeny of caveolin-1 heterozygote crosses. Probing of Xba I–digested DNA revealed 4.3- and 1.4-kb fragments for wild-type and disrupted genes, respectively. (+/+), (+/−), and (−/−) designate wild-type, heterozygous, and homozygous knockout animals, respectively. (**C**) RT-PCR of lung total RNA extracted from six littermate progeny of heterozygous crosses and amplified with primers specific for cav-1, -2, and -3. (**D**) Extracts of lungs (cav-1 and cav-2) or heart (cav-3) from (+/+), (+/−), and (−/−) animals were examined with antibodies directed against cav-1, cav-2, and cav-3. (**E**) Silver staining and GPI-anchored protein expression (as revealed by aerolysin overlay) in detergent-resistant membrane fractions from the lungs of (+/+) and (−/−) mice.

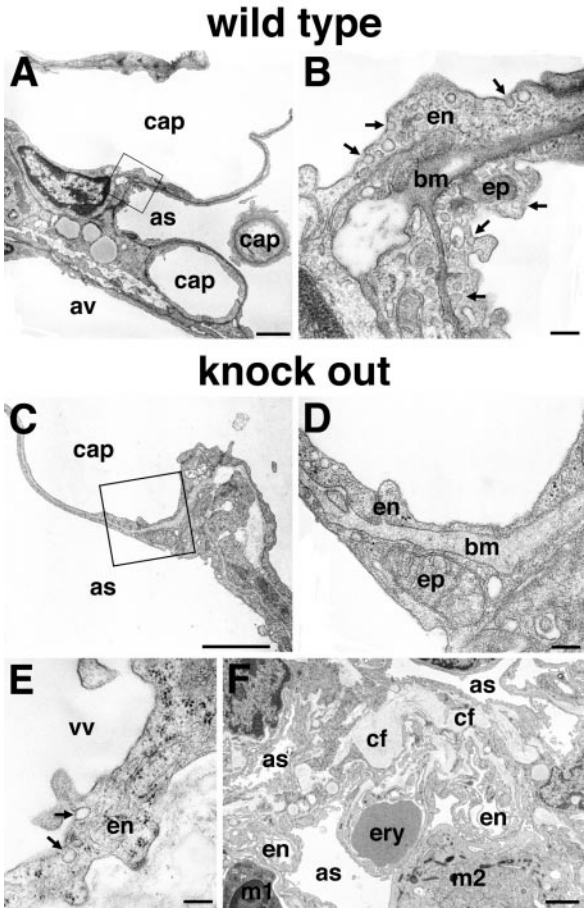

Fig. 2. Electron micrographs of lung tissue in (+/+) [(A) and (B)] and (−/−) [(C) to (F)] mice. The alveolae of wild-type mice showed the normal architecture (**A**) with the alveolar space (as) separated from the blood capillaries (cap) by the septum. The septum consists of a layer of epithelium (ep), the basal membrane (bm), and a layer of endothelium (en). av, arterial vessel. (**B**) High magnification of the inset in (A). Both the epithelial cells and the endothelial cells were covered with caveolae (arrows). (**C**) The caveolae have disappeared from both the epithelial and endothelial cells in (−/−) mice. (**D**) High magnification of the inset in (C). (**E**) Only in larger venous vessels (vv) were invaginations with a characteristic diaphragm observed. (**F**) Cav-1$^{-/-}$ mice displayed foci of septa with markedly altered architecture. In addition to the absence of caveolae, the capillaries showed deterioration of the endothelial layer and thickened connective tissue fibers (cf). Occasionally, septa contained trapped monocytes/macrophages (m1). m2 is a macrophage in the alveolar space. Bar, 10 μm [(A), (C), and (F)], 200 nm [(B), (D), and (E)].

normal in knockout animals.

The lack of caveolae in cav-$1^{-/-}$ mice offered the opportunity to address directly whether this organelle is involved in various signaling events. We focus here on nitric oxide (NO) signaling, calcium signaling, and tumor suppression.

We studied the role of caveolae in endothelium-dependent and NO-mediated vascular relaxation in isolated aortic rings (*24*, *25*). Rings derived from mutant mice failed to establish a steady contractile tone, with the vascular wall oscillating with a frequency of one per minute. Moreover, marked relaxation in the response to acetylcholine was observed. Whereas in wild-type animals the relaxation after precontraction with phenylephrine did not exceed 50%, in knockout animals the relaxation was complete (Fig. 3, A and B). To clarify if this difference was dependent on the NO pathway, we directly measured NO in primary cell culture of aortic vascular smooth muscle cells (VSMCs) with a selective microelectrode (*26*, *27*). The basal release of NO in cav-$1^{-/-}$ cells was 31% higher than in wild-type cells. Moreover, we compared downstream elements of the NO pathway and observed an about threefold higher content of cyclic guanosine monophosphate (cGMP, the major mediator of NO signaling) in knockout animals [cGMP content in fmol/g of tissue (mean ± SEM): 338.2 ± 56.5 (knockout) versus 108.3 ± 41.8 (wild type), $P < 0.02$]. Thus, cav-1 and caveolae are involved in the regulation of the NO pathway where NO synthases become hyperactivated in the absence of cav-1 (*24*, *27*).

Caveolae are also abundant in VSMCs. Despite the normal expression of muscle-specific cav-3, caveolae were absent from VSMCs in cav-$1^{-/-}$ animals. To study the consequences of caveolae deficiency, we measured the arterial response to vasoconstrictors. A manifold weaker calcium-dependent contractile response of arteries to angiotensin II, endothelin-1, and phorbol ester in cav-$1^{-/-}$ mice (Fig. 3E) was found. We also determined the myogenic tone of blood vessels, a partially contracted state that is an important determinant of blood pressure. This tone is regulated by a feedback mechanism tightly linking STOCs (spontaneous transient outward currents) to Ca^{2+} sparks (local increases in subsarcolemmal Ca^{2+}). Both are proposed to be dependent on the presence of caveolae (*28*). To determine whether this feedback mechanism is still functional in the absence of caveolae, we studied the frequency of STOCs in VSMCs and found that the STOCs were substantially (by a factor of ≤4, $P < 0.01$) reduced in the knockout animals at the physiological membrane po-

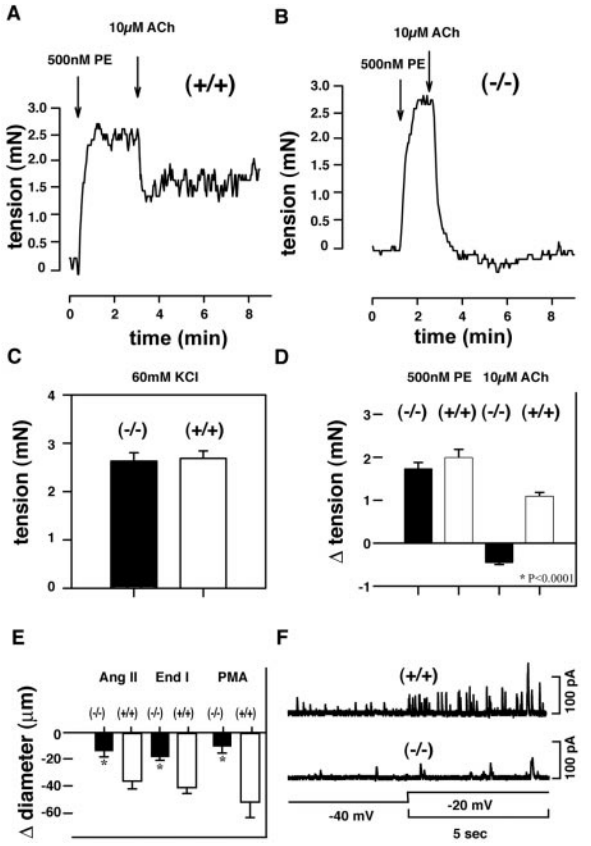

Fig. 3. (**A** and **B**) The acetylcholine (Ach)–induced relaxation of arteries was potentiated in cav-$1^{-/-}$ animals. (**C**) Thoracic aortic rings were treated with KCl to assess their functional integrity. (**D**) Aortic ring preparations of (−/−) ($n = 24$) and (+/+) ($n = 20$) mice showed a similar contractile response to 500 nM phenylephrine (PE). However, subsequent application of acetylcholine (10 μM) resulted in markedly stronger relaxation in (−/−) mice. (**E**) Contractile response of small arteries to vasoactive agonists. (**F**) Representative recordings of the spontaneous transient outward currents (STOCs, the myogenic tone determinant) in VSMCs, isolated from cerebral arteries of (+/+) and (−/−) animals. The frequency of STOCs in cav-$1^{-/-}$ was only 27% of that detected in cav-$1^{+/+}$ cells ($P < 0.01$).

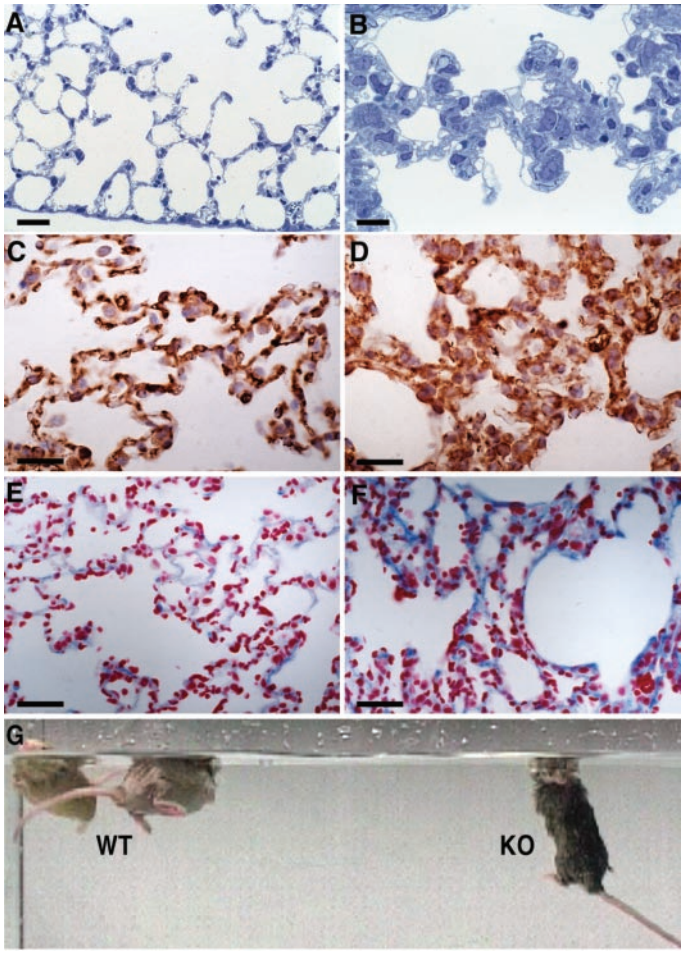

Fig. 4. Pathomorphological defects in lungs and physical disability of cav-$1^{-/-}$ animals. Paraffin sections of lung tissue from wild-type (**A**, **C**, and **E**) and cav-$1^{-/-}$ mice (**B**, **D**, and **F**) were (immuno)-stained with hematoxylin-eosin [(A) and (B)], antibody to Flk1 [(C) and (D)], or azan [(E) and (F)]. Substantial thickening of the alveolar wall is apparent in cav-$1^{-/-}$ mice [compare (A) and (B)], proliferation of Flk1-positive cells [compare (C) and (D)], and increased content of extracellular fibrillar matrix [compare (E) and (F)]. Bars, 20 μm. (**G**) Different swimming capabilities of cav-$1^{-/-}$ (KO) and wild-type (WT) mice after 15 min of the swimming test.

tential of −40 mV (Fig. 3F) (*29*).

Thus, the analysis of the aortic rings and the VSMCs shows that cav-1/caveolae regulate three major vascular features that depend on NO and Ca^{2+} signaling: endothelium-dependent relaxation of arteries, myogenic tone, and stimulated contractility.

The lack of caveolae also caused severe pathomorphological defects of lung alveolar septa, where gas exchange takes place. In knockout animals, large areas of the lungs (up to 30%) displayed markedly thickened septa (Figs. 2F and 4B). The normal double-layered alveolar architecture was replaced by a multilayered, disorganized tissue. These abnormal septa showed immunostaining for Flk1 (Fig. 4, C and D), a marker of nondifferentiated endothelial and hematopoietic progenitors, but not for von Willebrand factor, which labels later stages of endothelial cell differentiation. The increased cellular content in septa was accompanied by an increase of extracellular fibrillar deposits, as visualized by azan stain (Fig. 4, E and F; see also Fig. 2F). Thus, the loss of caveolae leads to the initiation of fibrosis. The accumulation of fibers in the alveolar interstitium of knockout animals was accompanied by a marked hypertrophy of type II pneumocytes. The observed uncontrolled hyperproliferation of angioblastic cells implies a function for cav-1/caveolae in the local control of cell proliferation, consistent with in vitro studies suggesting that caveolin-1 may act as a tumor suppressor (*8*).

We investigated the effects of vascular dysfunction and lung defects described above on the physical ability of cav-$1^{-/-}$ animals. Indeed, they displayed a markedly reduced ability to perform physical work, as assessed by a forced swimming stress (*30*). Whereas the control animals were able to swim for 1 to 1.5 hours at 34°C, cav-$1^{-/-}$ animals showed signs of exhaustion after 15 to 20 min (Fig. 4G).

Our study of cav-$1^{-/-}$ animals provides several important findings. First, the disruption of the cav-1 gene caused a loss of caveolae from all analyzed tissues, and hence generated a cell organelle knockout. Second, mutant animals displayed profound dysfunction of the vascular system and pronounced thickening of lung alvaeolar septa caused by an uncontrolled proliferation of endothelial cells and fibrosis. Surprisingly, such a marked change in plasma membrane structure and accompanying signaling disturbances caused by the deletion of this cellular organelle were not lethal. Possibly, some of the functions postulated for caveolae may be taken over by lipid rafts, which have been shown to play a key role in many signal transduction processes without the involvement of caveolae. It is also possible that the functions of caveolin-1 are compensated by other molecules. Nevertheless, the role of caveolae is essential for the normal functioning of the lungs and the cardiovascular system.

References and Notes

1. Reviewed in R. G. Parton, K. Simons, *Science* **269**, 1398 (1995).
2. Reviewed in R. G. Anderson, *Annu. Rev. Biochem.* **67**, 199 (1998).
3. G. E. Palade, *J. Appl. Phys.* **24**, 1424 (1953).
4. _____, *Anat. Rec.* **136**, 254 (1960).
5. E. J. Smart, Y. Ying, W. C. Donzell, R. G. Anderson, *J. Biol. Chem.* **271**, 29427 (1996).
6. R. G. Anderson, B. A. Kamen, K. G. Rothberg, S. W. Lacey, *Science* **255**, 410 (1992).
7. S. Li, J. Couet, M. P. Lisanti, *J. Biol. Chem.* **271**, 29182 (1996).
8. F. Galbiati *et al.*, *EMBO J.* **17**, 6633 (1998).
9. K. G. Rothberg *et al.*, *Cell* **68**, 673 (1992).
10. T. V. Kurzchalia *et al.*, *J. Cell Biol.* **118**, 1003 (1992).
11. M. Murata *et al.*, *Proc. Natl. Acad. Sci. U.S.A.* **92**, 10339 (1995).
12. S. Monier *et al.*, *Mol. Biol. Cell* **6**, 911 (1995).
13. All animal experiments were approved by local authorities in accordance with criteria outlined by the American Physiological Society. A 129/SvJ BAC library (Genome Systems) was screened with a reverse transcriptase–polymerase chain reaction (RT-PCR) probe derived from the murine caveolin-1 cDNA. The structure of a targeting plasmid is shown in Fig. 1A. Two 129/SvJ embryonic stem cell (Genome Systems) clones with targeted disruption of the cav-1 allele were injected into blastocysts from C57BL/6 mice; the resulting chimeric mice were crossed with C57BL/6 mice, and the heterozygous progeny were inbred to yield cav-$1^{-/-}$ mice. Routine PCR genotyping was performed. For the detection of tissue-specific transcripts by RT-PCR, adult mouse lung and heart were minced, and RNA was extracted, as directed by the manufacturer (Biotecx Laboratories). The reverse transcription was carried out with SuperScript II RNase H^- Reverse Transcriptase and random hexamers (Boehringer Mannheim). Antibodies used for Western blotting and inmunocytochemistry were as follows: anti–cav-1 (polyclonal C13630, Transduction Labs); anti–cav-2 (monoclonal C57820, Transduction Labs); anti–cav-3 [monoclonal C38320, Transduction Labs; vWF (A0082), Dako]; and monoclonal anti-flk1 (sc-6251, Santa Cruz). Samples for electron microscopy examination were fixed with glutaraldehyde and embedded in Epon according to standard protocols.
14. A. M. Fra, E. Williamson, K. Simons, R. G. Parton, *Proc. Natl. Acad. Sci. U.S.A.* **92**, 8655 (1995).
15. P. Scheiffele *et al.*, *J. Cell Biol.* **140**, 795 (1998).
16. T. V. Kurzchalia, R. G. Parton, *Curr. Opin. Cell Biol.* **11**, 424 (1999).
17. K. Simons, E. Ikonen, *Science* **290**, 1721 (2000).
18. T. Harder, P. Scheiffele, P. Verkade, K. Simons, *J. Cell Biol.* **141**, 929 (1998).
19. D. A. Brown, J. K. Rose, *Cell* **68**, 533 (1992).
20. L. Abrami, M. Fivaz, P. E. Glauser, R. G. Parton, F. G. van der Goot, *J. Cell Biol.* **140**, 525 (1998).
21. J. E. Schnitzer, P. Oh, D. P. McIntosh, *Science* **274**, 239 (1996).
22. The albumin concentration in cerebrospinal fluid was measured densitometrically after SDS-electrophoresis and staining with Fast Blue (Amersham Pharmacia Biotech, Piscataway, NJ). We used 99% globulin-free mouse albumin (Sigma, St. Louis) as a standard.
23. J. Babitt *et al.*, *J. Biol. Chem.* **272**, 13242 (1997).
24. M. Bucci *et al.*, *Nature Med.* **6**, 1362 (2000).
25. Aortic ring relaxation studies were done as described (*24*). In our experiments, aortic rings were treated with 500 nM phenylephrine and then with 10 μM acetylcholine. For measurements of the intracellular arterial wall Ca^{2+} concentration, the vessels were incubated with the Ca^{2+}-sensitive indicator fura-2/AM (5 μM).
26. H. Haller, C. Lindschau, P. Quass, A. Distler, F. C. Luft, *Circ. Res.* **76**, 21 (1995).
27. NO-selective microelectrode NO-release measurements were performed with an ISO-NOP 2-mm sensor connected to the ISO-NO Mark II Nitric Oxide Meter (World Precision Instruments, Sarasota, FL). The cGMP content in the lungs was estimated as directed by the manufacturer (Amersham Pharmacia Biotech, Piscataway, NJ).
28. M. Lohn *et al.*, *Circ. Res.* **87**, 1034 (2000).
29. S. Pluger *et al*, *Circ. Res.* **87**, E53 (2000).
30. The swimming test was performed at 34°C and documented by video recording.

31. We thank M. Strehle, V. Pevzner, and L. Li (Max-Delbrück-Center, Berlin, Germany) for advice on the embryonic stem cell manipulations, D. Landrock for help with the generation of chimeric mice, A. Henske and P. Quass (Max-Delbrück-Center, Berlin, Germany) for technical assistance, K. Margitudis (Max Planck Institute for Molecular Biology and Genetics, Dresden, Germany) for video recording, and F. Gisou van der Goot (Department of Biochemistry, University of Geneva, Switzerland) for providing aerolysin and performing aerolysin overlays. We are indebted to M. Zerial, M. Gonzales-Gaitan, and K. Simons (all from Max Planck Institute for Molecular Cell Biology and Genetics, Dresden, Germany) for critical reading of the manuscript and suggestions for improving it.

21 May 2001; accepted 30 July 2001
Published online 9 August 2001;
10.1126/science.1062688
Include this information when citing this paper.